Platelet integrins exhibit anisotropic mechanosensing and harness piconewton forces to mediate platelet aggregation

Yun Zhang[a,1], Yongzhi Qiu[b,c,d,1], Aaron T. Blanchard[b], Yuan Chang[a], Josh M. Brockman[b], Victor Pui-Yan Ma[a], Wilbur A. Lam[b,c,d,e,2], and Khalid Salaita[a,b,d,2]

[a]Department of Chemistry, Emory University, Atlanta, GA 30322; [b]Wallace H. Coulter Department of Biomedical Engineering, Emory University and Georgia Institute of Technology, Atlanta, GA 30332; [c]Department of Pediatrics, Division of Pediatric Hematology/Oncology, Aflac Cancer and Blood Disorders Center of Children's Healthcare of Atlanta, Emory University School of Medicine, Atlanta, GA 30322; [d]Winship Cancer Institute, Emory University, Atlanta, GA 30322; and [e]Parker H. Petit Institute of Bioengineering and Bioscience, Georgia Institute of Technology, Atlanta, GA 30332

Platelet aggregation at the site of vascular injury is essential in clotting. During this process, platelets are bridged by soluble fibrinogen that binds surface integrin receptors. One mystery in the mechanism of platelet aggregation pertains to how resting platelets ignore soluble fibrinogen, the third most abundant protein in the bloodstream, and yet avidly bind immobile fibrinogen on the surface of other platelets at the primary injury site. We speculate that platelet integrins are mechanosensors that test their ligands across the platelet–platelet synapse. To investigate this model, we interrogate human platelets using approaches that include the supported lipid bilayer platform as well as DNA tension sensor technologies. Experiments suggest that platelet integrins require lateral forces to mediate platelet–platelet interactions. Mechanically labile ligands dampen platelet activation, and the onset of piconewton integrin tension coincides with calcium flux. Activated platelets display immobilized fibrinogen on their surface, thus mediating further recruitment of resting platelets. The distribution of integrin tension was shown to be spatially regulated through two myosin-signaling pathways, myosin light chain kinase and Rho-associated kinase. Finally, we discovered that the termination of integrin tension is coupled with the exposure of phosphatidylserine. Our work reveals the highest spatial and temporal resolution maps of platelet integrin mechanics and its role in platelet aggregation, suggesting that platelets are physical substrates for one another that establish mechanical feedback loops of activation. The results are reminiscent of mechanical regulation of the T-cell receptor, E-cadherin, and Notch pathways, suggesting a common feature for signaling at cell junctions.

platelets | integrin | mechanobiology | molecular tension sensors

Platelet-to-platelet aggregation is vital for hemostasis (Fig. 1A). The major adhesion molecule involved in platelet aggregation at low shear conditions is the $\alpha_{IIb}\beta_3$-integrin receptor present at high density both in the plasma membrane and in α-granules (1). Despite its abundance, this integrin is maintained in an inactive state and ignores soluble ligands, such as fibrinogen and fibronectin within the bloodstream. However, upon activation, platelets at the primary injury site undergo inside–out triggering of their integrins and rapidly bind soluble fibrinogen (2). Receptor-bound fibrinogen then functions to recruit quiescent platelets from the bloodstream (3). While recruitment of platelets is accelerated and amplified in the presence of agonists such as adenosine diphosphate (ADP) and thrombin, surface-anchored fibrinogen is sufficient to trigger outside–in integrin activation, which leads to platelet activation, platelet-to-platelet cohesion, and initiation of clot formation (4).

Soluble fibrinogen is the third most abundant protein in blood plasma (2–4 mg/mL), and thus platelets must discriminate between soluble and membrane-bound fibrinogen with high fidelity. Previous work showed that fibrinogen displayed a lower binding affinity to platelet integrins compared with monomeric fibrin (5). In addition to this biochemical contribution, we here postulate that platelet integrins mechanically test their ligands to distinguish between soluble and immobilized states, thereby mediating the process of platelet cohesion. This hypothesis is supported by recent work showing that platelets are more activated when exposed to fibrinogen immobilized onto stiffer polymer scaffolds (4). Still, there is little understanding of how the mechanics of integrin ligands regulate the initiation of platelet activation. Elucidating how chemo-mechanical coupling aids in the recognition of immobilized ligands is central to understanding platelet aggregation.

Following initial recruitment and adhesion of a resting platelet from the bloodstream, it rapidly undergoes a well-defined signaling cascade (Ca^{2+} influx, degranulation, phosphatidylserine exposure, etc.) that leads to the application of contractile mechanical forces, creating a plug and sealing the injury site. Accordingly, a platelet must deliver precise contractile forces that are coordinated in space and time. For example, polymer pillar force sensor experiments showed that microclots containing tens of platelets apply a collective force of ~80 nN after exposure to immobilized ligand (6). Our previously reported atomic force microscopy (AFM)-based mechanical measurements revealed a contractile force of up to ~70 nN per platelet (7). Traction force microscopy (TFM) measurements suggested a cumulative force of ~34 nN per activated platelet (8). Taken together, these studies clearly confirm that platelets exert nanonewton (nN)

Significance

During initial growth of a clot, it is necessary for platelets to aggregate, which is mediated by binding fibrinogen molecules that bridge platelets through their integrin receptors. How platelet integrin receptors rapidly bind fibrinogen that is attached to the surface of another platelet but yet ignore soluble fibrinogen remains a mystery. This is difficult to understand since fibrinogen is the third most abundant protein in blood plasma. Here we show that differentiation between soluble and immobilized platelet ligands is mediated by mechanical forces. We demonstrate that the platelet integrins apply specific piconewton forces to test their ligands within the platelet junction. Our results provide insights into how clotting functions.
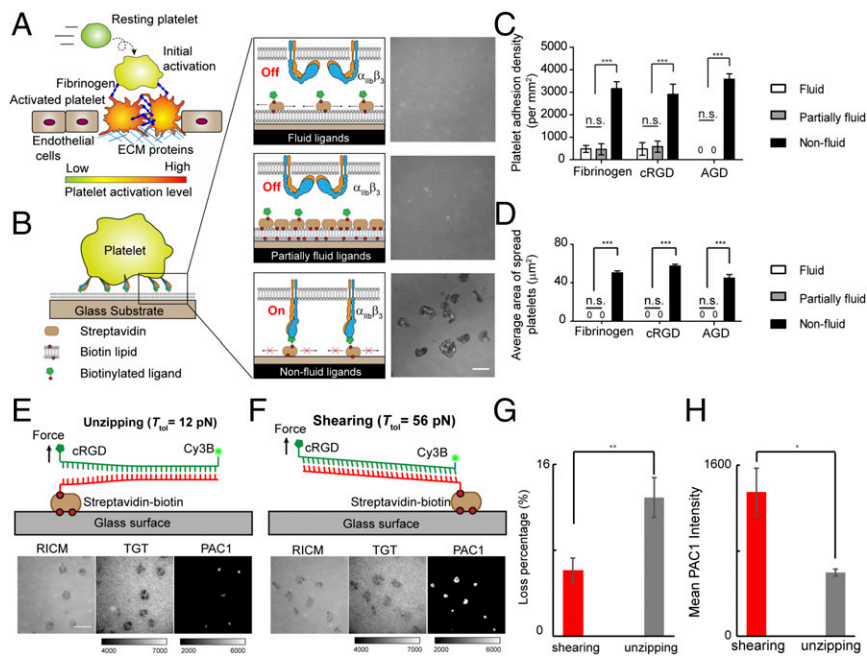
www.manaraa.com

Fig. 1. Ligand mechanics regulate initial platelet activation. (*A*) Schematic of primary clot recruitment of resting platelets. (*B*) Scheme of SLB platform used to study platelet activation. RICM images of human platelets interacting with SLBs of differing ligand fluidity. (Scale bar: 10 μm.) (*C*) Plot of platelet adhesion density and (*D*) platelet spreading area on SLBs with different ligand fluidity and ligand type (***$P < 0.001$; n.s.: not significant; $n = 3$ experiments, where each experiment was conducted on a separate substrate from which three images were collected and the average number of platelets was measured). The error bars indicate SD. (*E* and *F*) Schematic of 12- and 56-pN TGTs along with images showing platelet spreading, loss of TGT, and PAC-1 staining. (Scale bar: 10 μm.) (*G*) Bar graph quantifying the loss of fluorescent TGT for 12- and 56-pN probes. (*H*) Bar graph showing the average PAC-1 intensity for platelets on 12- and 56-pN TGTs. For *G* and *H*, the data were averaged from $n = 3$ experiments, where each experiment was conducted on a single substrate and three images were analyzed from each substrate. There were at least 20 platelets analyzed per group. The error bars indicate SD (**$P < 0.01$, *$P < 0.05$).

scale forces minutes following initial triggering. Given that the force resolution of TFM is at the nN scale, three orders of magnitude greater than the piconewton (pN) forces transmitted by integrin receptors, there is significant averaging of the signal, thus obscuring nascent, weak, or disorganized adhesion forces. Moreover, TFM resolves forces with ~1-μm spatial resolution, which is particularly problematic for studying platelet mechanotransduction because the size of platelets is ~2- to 3-μm. Although AFM is sensitive to pN forces, its application is limited because the technique is serial, which prevents mapping of forces across the cell surface. Therefore, current approaches are unable to image initial mechanical signaling events during platelet activation and subsequent aggregation. Mapping platelet forces with pN resolution and submicron spatial resolution is paramount to understanding the biophysical mechanisms of clot retraction and how mechanical stability of the clot is established, both of which are associated with pathological states when dysregulated (9, 10).

In this report, we recapitulated the platelet–platelet junction by immobilizing integrin ligands onto a supported lipid bilayer (SLB) with controlled mobility. These experiments show that platelets failed to activate on laterally fluid but axially fixed ligands, suggesting that platelet integrins display selective activation in response to tangential tension over forces that are in an orientation perpendicular to the substrate plane. Thus, ligand lateral mobility tunes ligand potency. In agreement with this result, we show that immobilizing integrin ligands using labile anchors dampens activation as measured by cell spreading and immunostaining. We found that, when a platelet is activated, it rapidly sequesters soluble fibrinogen from solution and transports the ligand into a central zone at the initial site of adhesive platelet–substrate contact. The centrally transported fibrinogen exhibits limited lateral mobility, thus placing it in an active mechanical state that should accelerate the recruitment of additional platelets. Next, we generate the first pN maps of integrin tension during platelet activation using our recently developed molecular tension probes. Our results demonstrate that integrin tension is associated with the earliest steps of platelet activation and coincides with Ca^{2+} flux. In addition, we demonstrate that the distribution of integrin tension is spatially regulated through two myosin-signaling pathways, myosin light chain kinase, and Rho-associated kinase. Finally, we discovered that the termination of platelet forces is highly coupled with the exposure of plasma membrane phosphatidylserine (PS). Since PS initiates

thrombin activation and fibrinogen polymerization into fibrin, this last observation suggests that cross-linking of platelets by fibrin is rapidly accelerated as platelets terminate their contractile phase of activation.

Results

Platelet Integrin Activation Requires Tangential Forces. Soluble fibrinogen molecules bind to the $\alpha_{IIb}\beta_3$ integrins on the surface of activated platelets at the primary injury site (3). Surface-bound fibrinogen molecules then, in turn, provide adhesion sites for recruiting inactive platelets from the blood stream, resulting in platelet aggregation and the generation of a growing thrombus (Fig. 1*A*). Knowing that platelets discriminate between soluble fibrinogen and immobilized ligands, we first asked how the lateral mobility of integrin ligands influences their potency for platelet triggering. The rationale was that membrane-anchored ligands confined to a 2D plane are amenable to clustering and oligomerization, which may enhance integrin activation.

To address this question, we mimicked the platelet–platelet junction by engaging human platelets to SLBs decorated with integrin ligands. The SLB is composed of phospholipids that are laterally mobile and modified with a variety of proteins, thus recapitulating the plasma membrane of a platelet (Fig. 1*B*) (11) . In our experiments, we decorated the SLB with integrin ligands, such as fibrinogen, cyclic-RGD (cRGD), and HHLGGAKQAGD (AGD) peptides. The cRGD and AGD peptides were synthesized and tested because they are minimal sequences obtained from the two adhesive motifs in the α- and γ-chains of fibrinogen, respectively, and have been shown to bind the $\alpha_{IIb}\beta_3$- integrin (*SI Appendix*, Figs. S1 and S2) (12–14). SLBs were formed by self-assembling lipids onto a glass slide, and ligands were then anchored onto the SLB through biotin–streptavidin binding to biotinylated lipids. Ligand density was maintained in all our surfaces, ~500 molecules/μm², based on quantitative fluorescence calibration (*SI Appendix*, Fig. S3) (15). When the biotinylated lipid density was 0.1%, the anchored ligands were fluid with a diffusion coefficient of ~1.3 μm²/s, as determined by fluorescence recovery after photobleaching (FRAP) (*SI Appendix*, Fig. S4 and Movie S1). In contrast, a 4% doping density of biotinylated lipids led to streptavidin crowding and a marked reduction in long-range ligand mobility, as shown previously (*SI Appendix*, Fig. S4) (11, 16). Platelet activation on fluid and partially fluid SLBs was compared with that of conventional

glass substrates on which the ligand was immobilized. We used platelet adhesion density and spreading areas as a proxy for platelet activation in accordance with the literature (4, 17).

When human platelets were incubated on the fluid SLBs for 20 min, there was minimal cell adhesion and no detectable platelet spreading, as measured using reflection interference contrast microscopy (RICM) (Fig. 1 *B–D* and Movie S2). Limiting long-range ligand mobility similarly resulted in no detectable platelet activation (Fig. 1 *B–D*). In contrast, when ligands at equivalent or lower density were immobilized on a fixed substrate, there was a drastic increase in platelet adhesion and spreading (Fig. 1 *B–D*). Pretreating platelets with ADP, an agonist that drives platelet aggregation, led to platelet spreading on the SLB surfaces, which is consistent with inside–out activation of integrins (*SI Appendix*, Fig. S5). Given that these surfaces present chemically identical ligands that differ only in their physical mobility, the data demonstrate that platelet integrins are mechanosensors. Moreover, SLBs offer little resistance to shear forces but strongly resist normal forces (18). Therefore, lateral forces are necessary for platelet integrin activation. Notably, our results are consistent with the conclusions of Springer and colleagues (19) stating that lateral forces are the most physiologically relevant mechanism for activating integrins. This conclusion was based on modeling showing that lateral forces applied to the integrin–ligand complex stabilize its high-affinity active state. This is in contrast to axial forces that seem to stabilize the low-affinity closed integrin conformation (4, 19, 20). Our results also agree with previous studies of nucleated cells showing that lateral resistance is necessary for the maturation of integrin adhesions (21, 22).

To further confirm the role of mechanics in platelet activation, cells were incubated on substrates coated with the recently reported DNA tension gauge tether (TGT) (23–25) to physically cap integrin $\alpha_{IIb}\beta_3$ tension (Fig. 1 *E* and *F*). The TGT is a DNA duplex designed to rupture at forces exceeding its "tension tolerance" (T_{tol}), defined as the force required to denature the duplex when a constant force is applied for less than 2 s. One DNA strand was modified with the cRGD peptide and a fluorescent reporter, while the complement was fixed onto the substrate. In this way, TGTs maintain the chemical recognition between the integrin and its ligand; however, the TGT sets the upper limit of forces experienced during mechanosensation. We challenged platelets with TGT constructs of T_{tol} values of 12 and 56 pN, which correspond to identical DNA sequences but differ in orientation, dissociating in either unzipping or shearing modes. Indeed, the weaker 12-pN TGT displayed more dissociation (twofold difference) compared with the 56-pN TGT probes (Fig. 1*G* and *SI Appendix*, Fig. S6). Platelet activation was quantified using PAC-1, an antibody that binds to the activated integrins $\alpha_{IIb}\beta_3$ (26). Platelets that adhered to the 56-pN (shearing) TGT displayed higher PAC-1 intensity compared with platelets spreading onto the 12-pN (unzipping) TGT (Fig. 1*H*). Capping the receptor force at 12 pN leads to dampening of platelet activation, likely by hampering the lifetime of the mechanical tension and also by limiting the peak tension. Thus, human platelet integrins mechanically test their integrin ligands using forces in the range of ∼12–56 pN.

Finely Tuned pN Forces Are Transmitted Through Individual Integrins in a Dynamic Spatiotemporal Pattern During Platelet Activation. The process of clot formation requires mechanical contraction of platelets following their aggregation (Fig. 2*A*). The magnitude and spatial/temporal distribution of integrin forces during platelet activation is unknown, and thus we used DNA-based molecular tension fluorescence microscopy (MTFM) to directly map integrin mechanics upon ligand binding (Fig. 2*B*) (15, 25, 27). In brief, MTFM probes consist of a DNA hairpin labeled with a Cy3B-BHQ2 fluorophore-quencher pair. One end of the probe was immobilized onto a glass slide, while the other terminus was coupled to the cRGD ligand. The DNA hairpin unfolds and generates a 34- ± 2-fold increase in fluorescence when the applied force exceeds the $F_{1/2}$ (defined as the force at which 50% of hairpins unfold at equilibrium). By varying the guanine-cytosine

(GC) content and stem-loop structure of the hairpins, $F_{1/2}$ can be tuned from 4.7 to 19.3 pN to visualize different magnitudes of integrin tension (Fig. 2*C*) (15, 28).

The cRGD probes with $F_{1/2}$ of 4.7 pN were first used to map tension dynamics spanning platelet activation from initial landing to spreading (Fig. 2*D* and Movie S3). Within minutes of cell seeding, the platelets engaged the surface as shown by RICM. Simultaneously, a punctate 4.7-pN tension signal was colocalized with RICM. Shortly thereafter, filopodia appeared in RICM, and was accompanied by tension radiating from the center to the edge of the filopodia. Once the filopodia became mature (∼4 min after initial contact), the platelet lamellipodia filled in the gaps between the filopodial projections and developed tension at the front of the growing lamellipodium. The spreading resulted in a ring of tension at the platelet perimeter. The lamellipodia, along with the tension signal, continued growing until platelets fully spread to a diameter of ∼10 μm within 10 min of the initial contact. In contrast to the dynamic lamellipodial tension signal, the central region maintained more static tension.

When the tension signal was integrated, the total intensity increased and then reached a plateau, which was maintained for 20–30 min (Fig. 2*E* and *SI Appendix*, Fig. S7) (7, 8). Radial distribution analysis of tension at steady state ($n = 15$ platelets) revealed two local peaks that were consistent with the lamellipodial ring pattern and a high-intensity central region that formed at the initial site of platelet–substrate contact (Fig. 2*F*). The lamellipodial tension signal accounted for ∼40% of the total, while the remaining signal was primarily localized at the central zone (Fig. 2 *E* and *F*). Subsequently, platelets displayed an abrupt and complete loss of tension, accompanied by a reduction in RICM contrast (Fig. 2*E*). Taken together, MTFM provides integrin tension maps with spatial and temporal resolution unachievable by conventional TFM and micropillar arrays and reveals that platelets generate a distinct mechanical architecture and spatiotemporal pattern during activation compared with that reported in nucleated cells such as fibroblasts, epithelial cells, and smooth muscle cells (29–31).

To better define the magnitude of integrin tension during platelet activation, we challenged platelets with probes of $F_{1/2} = 13.1$ and 19.3 pN (15, 28). Although platelets displayed similar levels of adhesion and spreading on these two probes, the mean tension signal per platelet was 60–70% weaker (Fig. 2*G*). This shows that a significant fraction of integrins transduce a force of less than 13.1 pN during platelet activation (Fig. 2*G*). Nonetheless, integrin forces are heterogeneous, and while the signal at the lamellipodial edge was diminished for the 13.1 and 19.3 pN probes, the central signal was maintained (Fig. 2*H*). Further image analysis showed that the ratio of the lamellipodial edge signal normalized to the total tension decreased from 0.32 ± 0.05 for the 4.7 pN probes to 0.15 ± 0.06 and 0.04 ± 0.02 for the 13.1 and 19.3 pN tension probes, respectively (*SI Appendix*, Fig. S8). These results show that a subset of integrins at the center of the platelet contact experience forces >19.3 pN.

Note that the AGD ligands only generated detectable signal with 3.0 pN probes, which may be due to the weaker affinity of the AGD compared with the cRGD and fibrinogen ligands (*SI Appendix*, Fig. S9). In contrast, full-length fibrinogen produced signal with the 4.7 pN probe (*SI Appendix*, Fig. S10 and Movie S4). However, this tension signal was diffuse and less quantitative because fibrinogen dimers can cross-link the biotinylated tension probes and each receptor may engage multiple DNA probes. Accordingly, all subsequent MTFM experiments were performed with the cRGD probe.

To further test the mechanosensor model of platelet adhesion, we simultaneously measured integrin tension and calcium flux, a proxy for platelet activation (Fig. 2 *I* and *J* and *SI Appendix*, Figs. S11 and S12 and Movie S5). We hypothesized that, if platelets mechanically test integrin ligands with pN forces as a mechanism of discrimination between soluble and immobile ligand, then we would expect to observe tension preceding early markers of platelet activation. Representative time-lapse images and
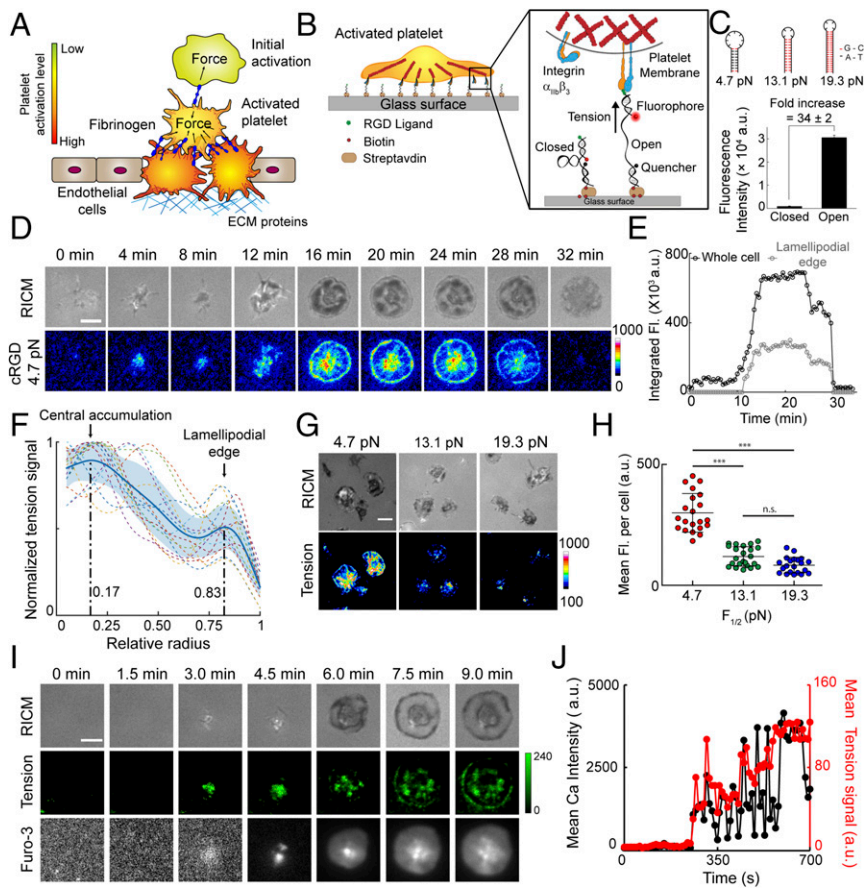
Zhang et al.

www.manaraa.com

Fig. 2. Platelets force mapping during adhesion and spreading. (*A*) Schematic of platelet–platelet junction through integrin $\alpha_{IIb}\beta_3$-fibrinogen complexes. (*B*) Scheme of DNA-based MTFM probes for integrin tension measurements. (*C*) Schematic of DNA hairpin structure, GC content, and $F_{1/2}$, along with fluorescence quenching efficiency measurements. (*D*) Time lapse of RICM and 4.7-pN tension map for single platelet. The fluorescence intensity shows the density of unfolded tension probes. (Scale bar: 3 μm.) (*E*) Integrated whole-platelet and lamellipodial fluorescence signal as a function of time for platelet in *D*. (*F*) Averaged tension radial intensity profile of 15 platelets analyzed from $n = 3$ substrates. (*G*) RICM and tension images for platelets engaged to probes with different $F_{1/2}$. (Scale bar: 5 μm.) (*H*) Histogram of mean platelet fluorescence intensity as a function of $F_{1/2}$. Each data point represents a single platelet. The data were collected from three experiments, where each experiment was conducted on a single substrate and there were at least 20 platelets analyzed for each group (***$P < 0.001$; n.s., not significant). The horizontal lines indicate the mean and SD. (*I*) Time-lapse images of RICM, 4.7-pN tension, and Ca^{2+} flux for platelets during initial activation. The Furo-3 images use adjusted contrasts to show early Ca^{2+} signal. (Scale bar: 3 μm.) (*J*) Plot quantifying tension and Ca^{2+} signals from a representative cell. More examples are shown in *SI Appendix*, Fig. S12.

quantitative analysis of a single platelet show that the initiation of integrin tension and calcium flux are synchronized within the temporal resolution of our experiments. Importantly, these data further support the mechanosensor model.

Following initial platelet aggregation, inside–out signaling leads to integrin binding of soluble fibrinogen, which is required for cross-linking of adjacent platelets. To examine the relationship between the pool of soluble and immobile integrin ligands, we exposed activated platelets to soluble alexa-488–labeled fibrinogen (10 μg/mL) and performed two-color time-lapse total internal reflection fluorescence microscopy (TIRFM) to map integrin tension and fibrinogen localization (*SI Appendix*, Fig. S13*A* and Movie S6). Soluble fibrinogen rapidly bound to the cell surface forming puncta that translocated along the basal face of the cell to the center of the cell–substrate junction. We tracked 45 fibrinogen clusters from $n = 9$ platelets and plotted their velocities over time. Cluster velocity decreased as fibrinogen moved toward the center of the platelet (*SI Appendix*, Fig. S13*B* and Movie S7). There was no significant change in integrin tension upon addition of soluble fibrinogen, suggesting minimal mechanical cross talk between these different pools of integrins. Finally, FRAP analysis showed that platelet-bound fibrinogen was immobile (*SI Appendix*, Fig. S13*C*), suggesting a mechanism in which soluble fibrinogen is bound and mechanically primed to recruit platelets from the bloodstream.

Spatial Distribution of Platelet Tension Is Regulated by Two Myosin-Signaling Pathways. Akin to nucleated cells, platelet forces are derived from myosin activity regulated by myosin light chain kinase (MLCK) and Rho-associated protein kinase (ROCK) (32). To clarify the role of these two kinases in platelet tension generation, we used inhibitors to interfere with myosin activity and measured integrin tension. Platelets were pretreated with 0.1% DMSO (vehicle control), MLCK inhibitor (10 μM ML-7), and ROCK inhibitor (30 μM Y27632) for 1 h and then incubated

on the 4.7-pN cRGD probe surfaces. After 20 min, platelets treated with Y27632 displayed diminished tension signal but stably adhered and spread onto substrates (Fig. 3 *A* and *B*). Platelets treated with ML-7 adhered to substrates but failed to spread and generate tension signal. Importantly, platelets treated with Y27632 lacked the strong central tension signal typical of untreated cells. Indeed, the ratio of lamellipodial edge signal over the total tension signal increased from 0.32 ± 0.06 to 0.44 ± 0.06 (Fig. 3*C*, $n = 20$). Radial intensity profiling of 25 platelets confirmed this result, showing a peak corresponding to the lamellipodial edge without the peak at the center of platelets (Fig. 3*D*).

To investigate the role of these two kinases following initial adhesion, we treated platelets with inhibitors after seeding the cells onto the surface for 20 min. ROCK inhibition led to a gradual decrease in the total tension signal as well as attenuation of the central tension zone in a period of 10 min (Fig. 3*E*). In contrast, MLCK inhibition dramatically reduced tension within ~1 min, eradicating signal within the lamellipodial region but sparing a small amount of central platelet-generated tension (Fig. 3*F* and Movie S8). Together, these results suggest that RhoA and MLCK kinase-signaling pathways have distinct roles in the spatial regulation of myosin activities and integrin forces. RhoA primarily drives the high-magnitude integrin forces at the center of the platelets, while MLCK is necessary for spreading, lamellipodia extension, and filopodial protrusion. Inhibiting MLCK abolishes remodeling of the cytoskeleton at the platelet periphery, which is critical for platelet spreading and formation of stable adhesions.

Correlation of PS Exposure with Platelet Tension. PS is a negatively charged lipid typically localized to the inner leaflet of the platelet membrane (33). PS exposure to the outer leaflet promotes platelet procoagulant activity and is also associated with the proteolysis of the cytoskeleton (Fig. 4*A*) (34, 35). However, the relationship between PS exposure and platelet tension remains
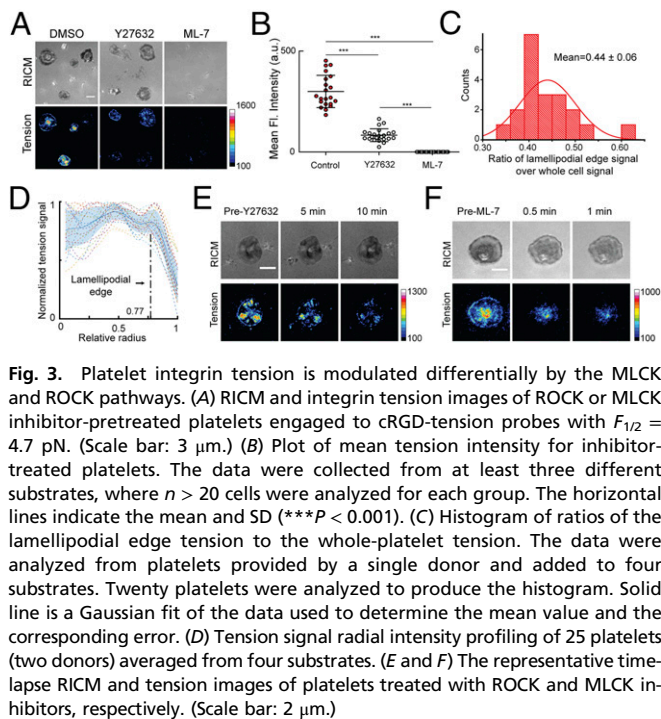
Fig. 3. Platelet integrin tension is modulated differentially by the MLCK and ROCK pathways. (*A*) RICM and integrin tension images of ROCK or MLCK inhibitor-pretreated platelets engaged to cRGD-tension probes with $F_{1/2}$ = 4.7 pN. (Scale bar: 3 μm.) (*B*) Plot of mean tension intensity for inhibitor-treated platelets. The data were collected from at least three different substrates, where $n > 20$ cells were analyzed for each group. The horizontal lines indicate the mean and SD (***$P < 0.001$). (*C*) Histogram of ratios of the lamellipodial edge tension to the whole-platelet tension. The data were analyzed from platelets provided by a single donor and added to four substrates. Twenty platelets were analyzed to produce the histogram. Solid line is a Gaussian fit of the data used to determine the mean value and the corresponding error. (*D*) Tension signal radial intensity profiling of 25 platelets (two donors) averaged from four substrates. (*E* and *F*) The representative time-lapse RICM and tension images of platelets treated with ROCK and MLCK inhibitors, respectively. (Scale bar: 2 μm.)

unclear. We performed time-lapse experiments measuring PS exposure and integrin tension using confocal microscopy. Platelets were incubated with annexin V-Alexa 488, which binds PS, and then allowed to engage the 4.7-pN tension probe surface. Interestingly, we found that the abrupt loss of tension signal 30–50 min after initial platelet adhesion (Fig. 2*D*) coincided with PS exposure (Fig. 4*B* and Movie S9). Analysis of the temporal delay (Δt) between the loss of tension and PS exposure showed a mean value of 14.7 s for n = 23 platelets (Fig. 4 *C* and *D* and *SI Appendix*, Fig. S14). This demonstrates that proteolysis of cytoskeleton and the resulting integrin tension cessation is upstream of PS exposure. Three-dimensional reconstruction of platelet morphology during this process showed that as integrin tension decreased and PS level mounted, cells rounded up. This result agrees with the reduction in RICM contrast (Fig. 2*D* and *SI Appendix*, Figs. S14 and S15). Therefore, PS exposure follows cytoskeletal reorganization and loss of integrin tension.

Discussion

By controlling ligand mobility and ligand mechanical resistance, we showed that chemically identical ligands display differential levels of potency in activating platelets. This shows that outside–in initial platelet activation requires mechanical tension. The platelet response is pseudobinary, and only laterally immobile

ligands trigger cell activation, suggesting that $\alpha_{IIb}\beta_3$ activation is an anisotropic mechanosensor (36). Our observation of force-dependent activation of platelet integrins qualitatively agrees with cadherin and integrin activation on fluid membranes in nuclear cells (21, 37). For example, Yu et al. (21) showed that focal adhesion maturation is dependent on lateral resistive forces within a fluid membrane. However, there are distinct differences in platelet adhesion and spreading compared with nucleated cells. At the time-scale of our image acquisitions, we did not detect platelet adhesion and spreading on fluid and partially fluid membranes, suggesting strong suppression of integrin activation on laterally fluid ligands. In contrast, nucleated cells, such as fibroblasts and epithelial cells, use integrins to adhere to mobile ligands presented on lipid membranes, forming activated integrin clusters (21). Likewise, cadherins can be triggered on fluid membranes in a kinetic nucleation process (21, 37).

Our results support a concept where platelets perform a mechanical checkpoint of their integrin ligands to determine whether to activate and adhere. It is likely that the mechanism mediating this observation is driven by mechanical stabilization of $\alpha_{IIb}\beta_3$-integrin in the open conformation that enhances ligand affinity (1). This type of response is well documented for $\alpha_5\beta_1$ and likely to be the case for $\alpha_{IIb}\beta_3$ (38). Normal forces are insufficient to activate platelets, thereby suggesting that platelet integrins require tangential forces to mediate platelet activation. Such a model has been proposed for the $\alpha_{IIb}\beta_3$ receptor (32) and for the T-cell receptor (39). The result of this mechanical testing is that low (lateral) mechanical resistance results in bond dissociation, while high resistance forces stabilize integrins in their active state, triggering activation.

Importantly, our mechanical checkpoint model may explain how platelets discriminate between soluble fibrinogen and platelet-bound fibrinogen. The mechanical resistance of fibrinogen is likely due to two parameters. First, soluble fibrinogen becomes immobile once bound to integrins on the surface of activated platelets. Second, fibrinogen rapidly polymerizes forming fibrin networks that exhibit significant mechanical stiffness (40). Both of these mechanisms likely contribute to enhancing the fidelity of mechanical testing of fibrinogen to avoid unintended platelet activation.

Platelet forces accumulate in two zones: a central region with greater tension and a ring of peripheral signal along the lamellipodial edge. This tension signal pattern resembles $\alpha_{IIb}\beta_3$-integrin receptor distribution in platelets spread on a fibrinogen-coated surface (41) and is distinct from the tension distribution in nucleated cells that lack a central region of tension. We also found that platelets produced a greater tension signal on cRGD peptide compared with AGD peptide, both of which are widely used in integrin $\alpha_{IIb}\beta_3$ studies. This difference in mechanical response may be due to the weaker affinity of the AGD ligand compared with the cRGD peptide. MLCK contributed to the integrin tension at the cell edge, similar to its function in nucleated cells. Interestingly, ROCK inhibition in nucleated cells leads to the loss of stable focal adhesions and central stress fibers (42); in contrast, ROCK regulates the central contractile forces in
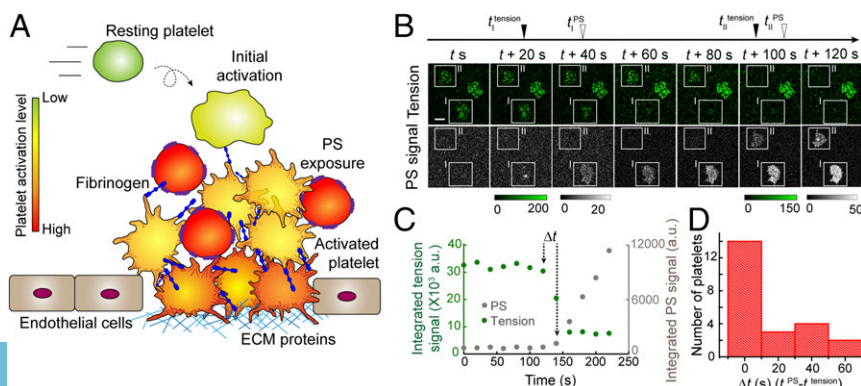
Fig. 4. Cessation of platelet tension coincides with PS exposure. (*A*) Schematic of PS exposure on platelets within a clot. (*B*) Time-lapse images of platelet tension and PS exposure on surface presenting 4.7-pN tension probes. Annexin V-Alexa 488 was used to stain for PS. Regions of interest (ROIs) I and II highlight two platelets during tension termination and PS exposure. The third platelet in the middle did not generate a detectable PS signal. (Scale bar: 2 μm.) (*C*) A plot of tension and PS intensity for ROI I in *B*. The term "Δt" is defined as the time difference between the time points of tension cessation and PS exposure. (*D*) The histogram of Δt indicates that tension disappearance is concurrent with PS exposure; n = 23 cells from three experiments.

platelets but did not abolish tension signal. Note that the central zone of tension was not reported in previous TFM measurements (8). This is likely due to the low spatial resolution of TFM and its inability to read out forces normal to the substrate.

Whereas biological agonists such as thrombin, ADP, and epinephrine are known to activate platelet aggregation, our data show that the mechanical microenvironment plays a role in this process as well. Specifically, the data suggest that fibrinogen anchoring results in a positive feedback loop of platelet activation, which may further drive platelet aggregation contributing to the presence of groups of highly activated platelets within a nascent clot.

Using DNA-based probes, we show that the magnitude of tension generated by platelet integrins ranges from 4.7 to 19.3 pN with a subpopulation that exceeds 19.3 pN. *SI Appendix,* Table S3 summarizes reported integrin traction forces in nucleated cells and *SI Appendix,* Fig. S16 compares integrin traction forces in nucleated cells and platelets. Previous papers reporting on the contractile forces applied by single platelets indicate forces of 29 nN (AFM) and 34 nN (TFM) (7, 8). By estimating the number of hairpins unfolded by a single platelet, we calculate that the force per cell is between ~6 and ~24 nN, which is consistent with prior reports. Note that this is a lower limit of the total tension since values below $F_{1/2}$ are not detected and forces exceeding $F_{1/2}$ are underestimated.

We also determined the temporal relationship between PS exposure, a prerequisite for platelet-dependent thrombin generation, and mechanical signaling. PS presentation rapidly follows the termination of platelet contraction, suggesting that PS-exposing cells do not actively contribute to the clot retraction process. Therefore, the release of tension by PS-positive platelets may relax the strained clot. As fibrinolysis can be retarded in the strained clot, our results suggest that PS-positive platelets not only play a biochemical role in clot fibrinolysis, but also mechanically contribute to fibrinolysis.

Materials and Methods

The whole-blood samples were obtained from healthy blood donors, and consent was obtained according to the protocol (H15258) approved by the Institutional Review Board at Georgia Tech. Whole blood was drawn into collection tubes with acid citrate dextrose (ACD). Platelet-rich plasma (PRP) was collected after centrifugation under $150 \times g$ for 15 min. Additional ACD was added into PRP (10% of the PRP volume), which was then centrifuged at $900 \times g$ for another 5 min. Platelet-poor plasma was then removed, and the platelet pellet was resuspended in Tyrode's buffer containing 0.1% BSA.

More detailed information about the materials and methods used in this study is provided in *SI Appendix, SI Materials and Methods.*

1. Bennett JS (2005) Structure and function of the platelet integrin alphaIIbbeta3. *J Clin Invest* 115:3363–3369.
2. Li Z, Delaney MK, O'Brien KA, Du X (2010) Signaling during platelet adhesion and activation. *Arterioscler Thromb Vasc Biol* 30:2341–2349.
3. Bennett JS (2001) Platelet-fibrinogen interactions. *Ann N Y Acad Sci* 936:340–354.
4. Qiu Y, et al. (2014) Platelet mechanosensing of substrate stiffness during clot formation mediates adhesion, spreading, and activation. *Proc Natl Acad Sci USA* 111:14430–14435.
5. Litvinov RI, Farrell DH, Weisel JW, Bennett JS (2016) The platelet integrin αIIbβ3 differentially interacts with fibrin versus fibrinogen. *J Biol Chem* 291:7858–7867.
6. Liang XM, Han SJ, Reems JA, Gao D, Sniadecki NJ (2010) Platelet retraction force measurements using flexible post force sensors. *Lab Chip* 10:991–998.
7. Lam WA, et al. (2011) Mechanics and contraction dynamics of single platelets and implications for clot stiffening. *Nat Mater* 10:61–66.
8. Schwarz Henriques S, Sandmann R, Strate A, Köster S (2012) Force field evolution during human blood platelet activation. *J Cell Sci* 125:3914–3920.
9. Tran R, et al. (2013) Biomechanics of haemostasis and thrombosis in health and disease: From the macro- to molecular scale. *J Cell Mol Med* 17:579–596.
10. Myers DR, et al. (2017) Single-platelet nanomechanics measured by high-throughput cytometry. *Nat Mater* 16:230–235.
11. Narui Y, Salaita K (2013) Membrane tethered delta activates notch and reveals a role for spatio-mechanical regulation of the signaling pathway. *Biophys J* 105:2655–2665.
12. Sánchez-Cortés J, Mrksich M (2009) The platelet integrin alphaIIbbeta3 binds to the RGD and AGD motifs in fibrinogen. *Chem Biol* 16:990–1000.
13. Srinivasan R, Marchant RE, Gupta AS (2010) In vitro and in vivo platelet targeting by cyclic RGD-modified liposomes. *J Biomed Mater Res A* 93:1004–1015.
14. Kononova O, et al. (2017) Mechanistic basis for the binding of RGD- and AGDV-peptides to the platelet integrin αIIbβ3. *Biochemistry* 56:1932–1942.
15. Zhang Y, Ge C, Zhu C, Salaita K (2014) DNA-based digital tension probes reveal integrin forces during early cell adhesion. *Nat Commun* 5:5167.
16. Ma VPY, et al. (2016) Ratiometric tension probes for mapping receptor forces and clustering at intermembrane junctions. *Nano Lett* 16:4552–4559.
17. Zou Z, Chen H, Schmaier AA, Hynes RO, Kahn ML (2007) Structure-function analysis reveals discrete beta3 integrin inside-out and outside-in signaling pathways in platelets. *Blood* 109:3284–3290.
18. Glazier R, Salaita K (2017) Supported lipid bilayer platforms to probe cell mechanobiology. *Biochim Biophys Acta* 1859:1465–1482.
19. Nordenfelt P, Elliott HL, Springer TA (2016) Coordinated integrin activation by actin-dependent force during T-cell migration. *Nat Commun* 7:13119.
20. Zhu J, et al. (2008) Structure of a complete integrin ectodomain in a physiologic resting state and activation and deactivation by applied forces. *Mol Cell* 32:849–861.
21. Yu CH, Law JBK, Suryana M, Low HY, Sheetz MP (2011) Early integrin binding to Arg-Gly-Asp peptide activates actin polymerization and contractile movement that stimulates outward translocation. *Proc Natl Acad Sci USA* 108:20585–20590.
22. Yu CH, et al. (2013) Integrin-matrix clusters form podosome-like adhesions in the absence of traction forces. *Cell Rep* 5:1456–1468.
23. Wang X, Ha T (2013) Defining single molecular forces required to activate integrin and notch signaling. *Science* 340:991–994.
24. Ma VP, et al. (2016) Mechanically induced catalytic amplification reaction for readout of receptor-mediated cellular forces. *Angew Chem Int Ed* 55:5488–5492.
25. Liu Y, et al. (2016) DNA-based nanoparticle tension sensors reveal that T-cell receptors transmit defined pN forces to their antigens for enhanced fidelity. *Proc Natl Acad Sci USA* 113:5610–5615.
26. Shattil SJ, Hoxie JA, Cunningham M, Brass LF (1985) Changes in the platelet membrane glycoprotein IIb.IIIa complex during platelet activation. *J Biol Chem* 260:11107–11114.
27. Liu Y, Galior K, Ma VP-Y, Salaita K (November 21, 2017) Molecular tension probes for imaging forces at the cell surface. *Acc Chem Res*, 10.1021/acs.accounts.7b00305.
28. Blakely BL, et al. (2014) A DNA-based molecular probe for optically reporting cellular traction forces. *Nat Methods* 11:1229–1232.
29. Chang Y, et al. (2016) A general approach for generating fluorescent probes to visualize piconewton forces at the cell surface. *J Am Chem Soc* 138:2901–2904.
30. Liu Y, Yehl K, Narui Y, Salaita K (2013) Tension sensing nanoparticles for mechano-imaging at the living/nonliving interface. *J Am Chem Soc* 135:5320–5323.
31. Munevar S, Wang Y, Dembo M (2001) Traction force microscopy of migrating normal and H-ras transformed 3T3 fibroblasts. *Biophys J* 80:1744–1757.
32. Calaminus SDJ, et al. (2007) MyosinIIa contractility is required for maintenance of platelet structure during spreading on collagen and contributes to thrombus stability. *J Thromb Haemost* 5:2136–2145.
33. Lentz BR (2003) Exposure of platelet membrane phosphatidylserine regulates blood coagulation. *Prog Lipid Res* 42:423–438.
34. Bevers EM, Comfurius P, Zwaal RF (1991) Platelet procoagulant activity: Physiological significance and mechanisms of exposure. *Blood Rev* 5:146–154.
35. Heemskerk JW, Siljander PR, Bevers EM, Farndale RW, Lindhout T (2000) Receptors and signalling mechanisms in the procoagulant response of platelets. *Platelets* 11:301–306.
36. Brockman JM, et al. (2017) Mapping the 3D orientation of piconewton integrin traction forces. *Nat Methods*, 10.1038/NMETH.4536.
37. Biswas KH, et al. (2015) E-cadherin junction formation involves an active kinetic nucleation process. *Proc Natl Acad Sci USA* 112:10932–10937.
38. Kong F, García AJ, Mould AP, Humphries MJ, Zhu C (2009) Demonstration of catch bonds between an integrin and its ligand. *J Cell Biol* 185:1275–1284.
39. Kim ST, et al. (2009) The alphabeta T cell receptor is an anisotropic mechanosensor. *J Biol Chem* 284:31028–31037.
40. Brown AE, Litvinov RI, Discher DE, Purohit PK, Weisel JW (2009) Multiscale mechanics of fibrin polymer: Gel stretching with protein unfolding and loss of water. *Science* 325:741–744.
41. Jirousková M, Jaiswal JK, Coller BS (2007) Ligand density dramatically affects integrin alpha IIb beta 3-mediated platelet signaling and spreading. *Blood* 109:5260–5269.
42. Liu Y, et al. (2014) Nanoparticle tension probes patterned at the nanoscale: Impact of integrin clustering on force transmission. *Nano Lett* 14:5539–5546.

www.manaraa.com